03,05,08

Magnetic properties of submicron α-Fe_2O_3 layers grown on sapphire by mist-CVD

© P.V. Kharitonskii[1], V.I. Nikolaev[1], R.B. Timashov[1], A.I. Stepanov[1], M.P. Shcheglov[1], K.G. Gareev[1,2,¶], A.Yu. Ralin[3], E.S. Sergienko[1,4]

[1] Ioffe Institute,
St. Petersburg, Russia
[2] St. Petersburg State Electrotechnical University „LETI",
St. Petersburg, Russia
[3] Far Eastern Federal University,
Vladivostok, Russia
[4] St. Petersburg State University,
St. Petersburg, Russia

E-mail: kggareev@yandex.ru

Received March 6, 2025
Revised March 6, 2025
Accepted May 5, 2025

Magnetic properties of submicron iron (III) oxide layers deposited by mist-CVD epitaxy on a sapphire substrate of basal orientation (0001) with and without a 2*H*-GaN buffer layer were studied. It was shown that both layers are close in composition to α-Fe_2O_3 (hematite). The presence of the GaN buffer layer leads to an increase in the saturation magnetization and saturation remanence. Magnetometry and magnetic force microscopy data allowed theoretical estimates to be made indicating the presence of vortex magnetic structures in the studied layers.

Keywords: Iron oxide, hematite, maghemite, gallium nitride, submicron layers, sapphire, mist-CVD, magnetic hysteresis, magnetic states, vortex structures.

DOI: 10.61011/PSS.2025.07.61882.23HH-25

1. Introduction

Polymorphic modifications of iron-III oxide (α-, β-, γ- and ε-Fe_2O_3) are referred as dilute magnetic semiconductors or dielectrics [1,2], which in the form of thin films are promising for spintronics, magneto-optics, photoelectrochemical water purification, etc., due to the wide band gap, high concentration of charge carriers of *n*-type, high Curie temperature, environmental safety and manufacturability (see, for example, [3,4]).

It is known [5] that bulk hematite samples (α-Fe_2O_3) containing submicron crystals with linear dimensions $0.12-0.45\,\mu$m have high values of the coercive force $H_c = 150-350$ mT at room temperature, while values $H_c = 0.8-23.0$ mT (in the basal plane) for crystals with dimensions $1.0-5.5$ mm. Hematite crystals owe their high value of H_c mainly to magnetoelastic anisotropy caused by internal stresses in small particles, and defects such as dislocations in large particles where stress relaxation has occurred. The ratio of the remanent saturation magnetization M_{rs} to saturation magnetization M_s for hematite in the single-domain (SD) state $M_{rs}/M_s = 0.5-0.7$, which differs slightly from the ratio in the multi-domain (MD) state $M_{rs}/M_s = 0.5-0.9$. At the same time, the values of the ratio of the coercive force in terms of remanent magnetization H_{cr} to the coercive force H_c significantly differ: SD — $H_{cr}/H_c = 1.5-1.6$; MD — $H_{cr}/H_c = 1.0-1.2$. It is also shown in Ref. [5] that the threshold size of the SD state ranges from $15\,\mu$m to several dozens of μm, but probably does not reach the value of $100\,\mu$m.

Based on the results of constructing FORC (First Order Reverse Curve) diagrams for synthesized and natural bulk samples containing hematite crystals, it is shown that in a zero external field, the presence of vortex structures (single vortex, SV state) is unlikely. Unlike bulk samples, vortex structures often occur in thin layers of hematite, for example, in epitaxial films of hematite with a thickness of 10 nm deposited by magnetron sputtering on sapphire with a buffer layer of Co(1 nm)/Al(1 nm) [7].

The purpose of this paper was to study the magnetic properties of submicron layers of iron oxides obtained by ultrasonic vapor chemical epitaxy (mist-CVD) on a sapphire substrate of basal orientation (0001) without a buffer layer and with a buffer layer of gallium nitride.

2. Materials and methods

Submicron layers of iron oxides in samples Fe_2O_3/Al_2O_3 and $Fe_2O_3/GaN/Al_2O_3$ was deposited by ultrasonic vapor chemical epitaxy (mist-CVD) in a reactor of its own design [8]. The thin layers were grown from an aqueous solution of iron acetylacetonate ($Fe(acac)_3$). The solution was sputtered with ultrasonic emitters (frequency 2.4 MHz) and supplied as droplets $10-100$ nm to the reactor with transport gas (argon), which supplied oxygen. The ratio of

their flows was 2 : 1. Sputtering took place on a sapphire substrate of basal orientation (0001) with and without a buffer layer 2*H*-GaN. The temperature in the growth zone was 500 °C.

Microscopic studies were performed using a scanning electron microscope (SEM) „Zeiss Merlin“ (Carl Zeiss AG, Germany) with a field emission cathode, an electron optics column „GEMINI-II“ and an oil-free vacuum system. The SEM images were obtained using a backscattered electron detector. The analysis of the elemental composition was performed using the built-in analytical console for electron microprobe analysis (EDX). The phase composition was characterized by X-ray diffraction using „DRON 8“ diffractometer („Burevestnik“, Russia). The hysteresis curves were constructed using a vibrating sample magnetometer „LakeShore 7410“ (Lake Shore Cryotronics Inc., USA) at a temperature of 295 K when magnetized parallel to the plane of the layer. To visualize the distribution of magnetic fields (observation of the domain structure), the method of magnetic force microscopy (MFM) was used in dynamic (semi-contact) mode in „INTEGRA-AURA“ system (NT-MDT, Russia). The theoretical analysis of the magnetic properties of the sample was carried out based on the approaches of micromagnetism and magnetic granulometry (see, for example, [9]).

3. Results and discussion

The SEM images of the obtained layers are shown in Figure 1. The characteristic sizes of crystals, probably iron oxides (the light areas in the images) are shown in Figure 1, *a* and Figure 1, *b*. Figure 1, *c* demonstrates the boundary region of a continuous iron oxide layer in the sample $Fe_2O_3/GaN/Al_2O_3$.

Iron oxide crystals in Fe_2O_3/Al_2O_3 (Figure 1, *a*) have a fine-grained, nanoscale structure. They are characterized by a heterogeneous morphology, have an irregular shape, often close to a polyhedral (polyhedral) structure with rounded edges and smoothed corners. The linear size of crystals is about 100 nm. They form accretions in a columnar structure, which may be related to the growth conditions of the layer, and are distributed evenly over the surface, forming a continuous densely packed nanostructured layer with a high degree of aggregation. Discontinuities and boundaries are observed between individual crystals, which can affect the magnetic and physico-chemical properties of the material.

The crystals also have a polyhedral (polyhedral) in the sample $Fe_2O_3/GaN/Al_2O_3$ (Figure 1, *b*), but a more rounded shape with an average size of 120–140 nm. The crystals are packed tightly (see Figure 1, *c*), forming a continuous granular structure, that is, the exchange interaction affects the magnetic state of the entire layer. It can be seen that the iron oxide crystals do not form a monolayer structure and are arranged in several levels. Local voids between crystals

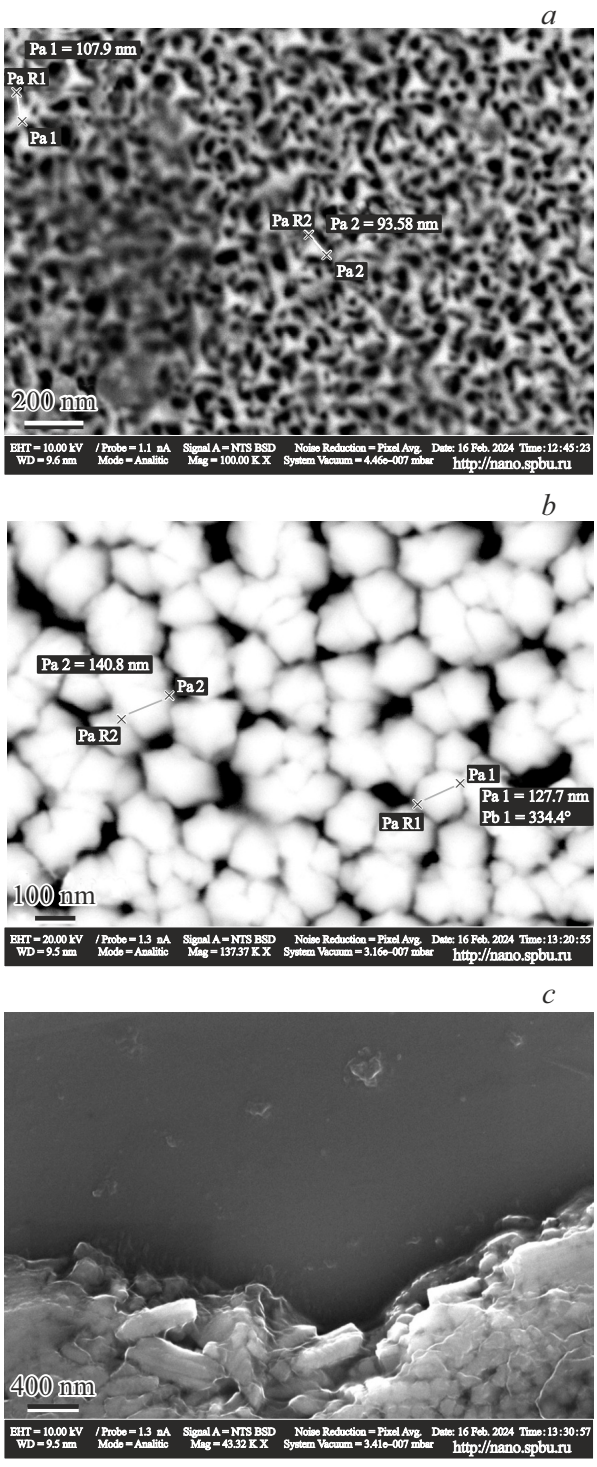

Figure 1. SEM images of the received layers: Fe_2O_3/Al_2O_3 (*a*); $Fe_2O_3/GaN/Al_2O_3$ (*b* — general view and *c* — view at the edge of the sample).

are observed, which may indicate diffusion processes at the deposition stage.

The results of the elemental composition analysis are listed in Table 1. The obtained oxygen-iron ratio corresponds to iron-III oxide for the sample Fe_2O_3/Al_2O_3. Anal-

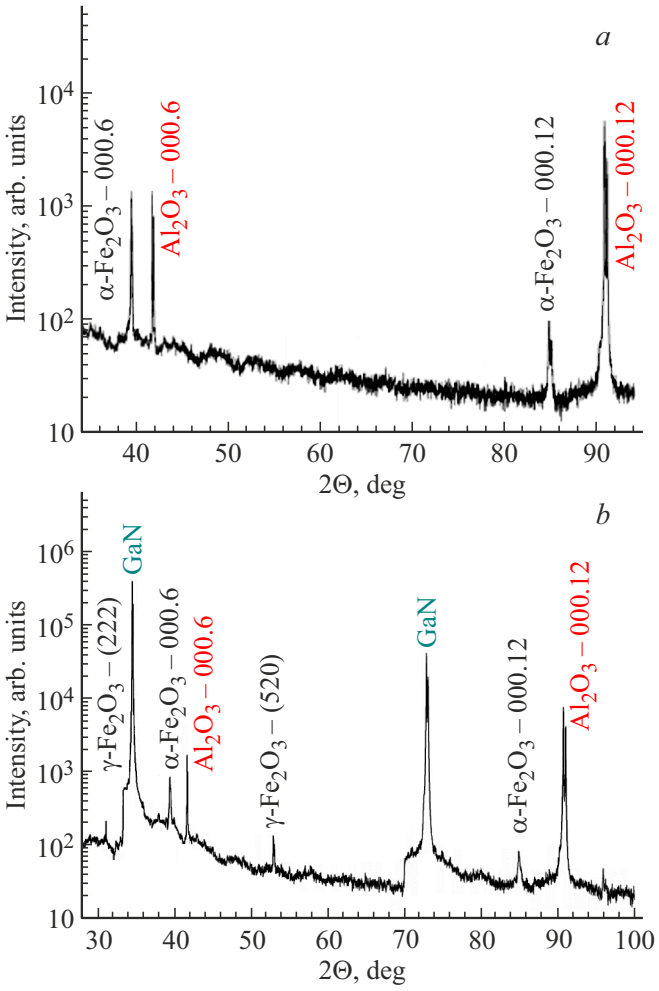

Figure 2. X-ray diffraction patterns of the obtained layers: *a* — Fe_2O_3/Al_2O_3; *b* — $Fe_2O_3/GaN/Al_2O_3$.

ysis of the $Fe_2O_3/GaN/Al_2O_3$ sample shows an increased oxygen content. This may be due to several reasons. Firstly, light elements, such as oxygen, are not always accurately analyzed in EDX and may be overestimated due to nitrogen being close in mass. Secondly, oxygen can additionally be detected from the substrate or other compounds present.

Table 1. Elemental composition of the outer surface layer of samples of Fe_2O_3/Al_2O_3 and $Fe_2O_3/GaN/Al_2O_3$, obtained by the EDX method

Chemical element	Atomic fraction,%	
	Fe_2O_3/Al_2O_3	$Fe_2O_3/GaN/Al_2O_3$
Fe	39.94	24.28
O	60.06	70.15
Ga	0.00	5.57

X-ray diffraction patterns of the studied layers are shown in Figure 2. The layer on the sapphire without buffer (Figure 2, *a*) has signs of only a trigonal structure — hematite (α-Fe_2O_3), whereas in the iron oxide layer, in the presence of a GaN buffer layer (Figure 2, *b*), the phases of hematite and maghemite (γ-Fe_2O_3) coexist.

MFM images of the surface of the iron oxide layer of the samples are shown in Figure 3 in a three-dimensional reconstruction. Variations in magnetic contrast are visible, which indicates the presence of inhomogeneous magnetic regions. A complex but ordered magnetic structure characterized by a combination of longitudinally oriented bands and localized heterogeneous areas is recorded for the sample of Fe_2O_3/Al_2O_3 (Figure 3, *a*). This configuration of magnetic separation may be due to the crystallographic features of the growth of Fe_2O_3 on a sapphire substrate Al_2O_3, as well as the influence of internal mechanical stresses and defects. Localized magnetic regions with varying contrast are recorded in Figure 3, *b* for the sample $Fe_2O_3/GaN/Al_2O_3$. Unlike the sample Fe_2O_3/Al_2O_3, these regions have a chaotic distribution, which may be due to the presence of ferrimagnetic regions γ-Fe_2O_3 (maghemite), their interphase interaction with α-Fe_2O_3 (hematite) and the effect of the GaN substrate.

Figure 4 shows the hysteresis curves for samples obtained at room temperature with and without correction for diamagnetism of the sapphire substrate (gray curve), as well as the curves of destruction of the remanent saturation magnetization M_{rs} (shown in the insets in the lower right corner).

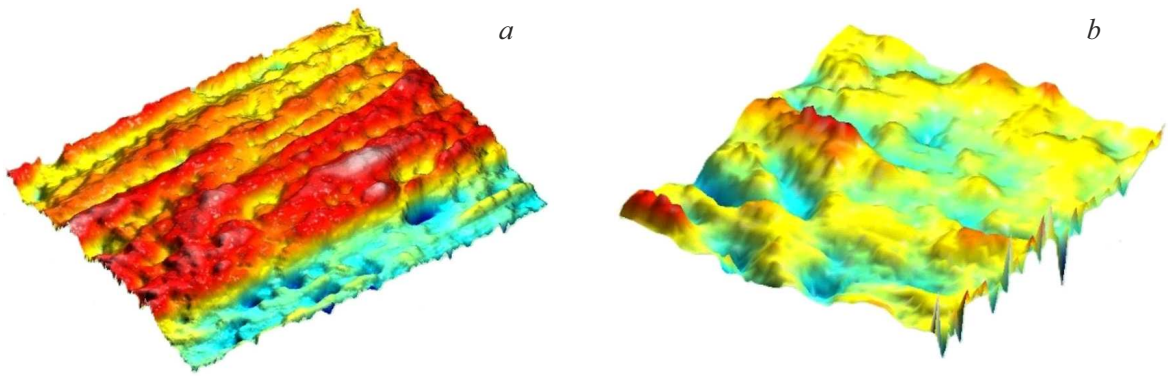

Figure 3. Three-dimensional reconstruction of MFM data: *a* — Fe_2O_3/Al_2O_3; *b* — $Fe_2O_3/GaN/Al_2O_3$. Scan area dimensions $20 \times 20\,\mu$m.

Table 2. Hysteresis parameters of iron oxide layers

Sample	$\mu_0 H_c$, mT	$\mu_0 H_{cr}$, mT	M_s, mA · m^2/kg	M_{rs}, mA · m^2/kg	H_{cr}/H_c	M_{rs}/M_s
Fe_2O_3/Al_2O_3	5	6	33	2	1.2	0.06
$Fe_2O_3/GaN/Al_2O_3$	4	6	46	4	1.5	0.09

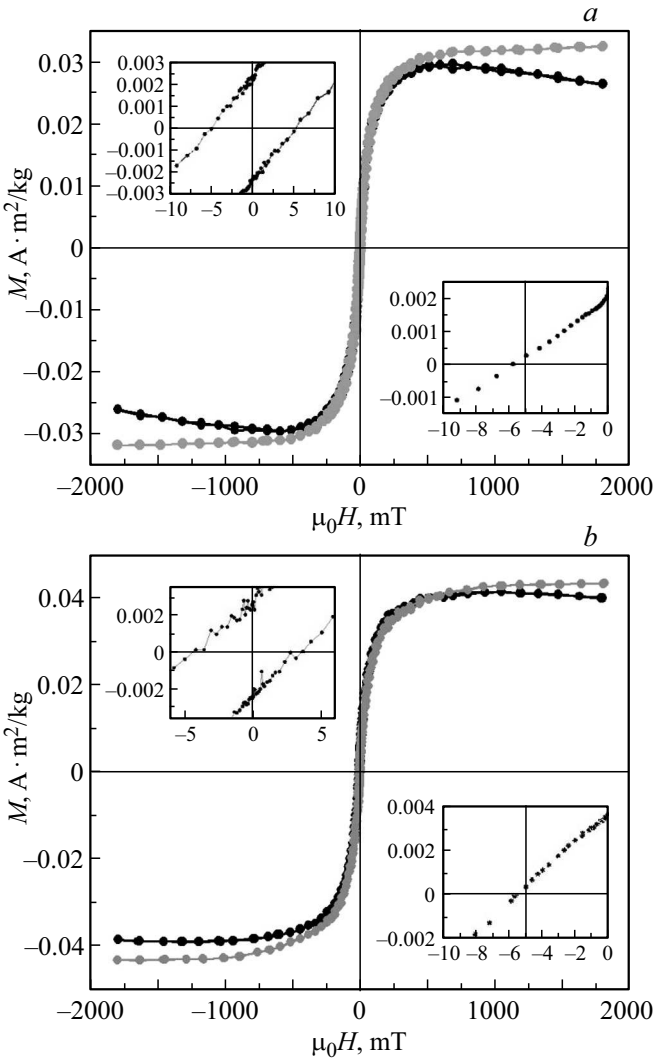

Figure 4. Hysteresis and DCD curves of remanent saturation magnetization M_{rs} for layers: *a* — Fe_2O_3/Al_2O_3; *b* — $Fe_2O_3/GaN/Al_2O_3$; central regions of the hysteresis loops are shown in the insets in the upper left corner. The direction of the external field is parallel to the layer.

The hysteresis parameters and magnetic-granulometric ratios for the studied samples are provided in Table 2.

The difference in crystal shape in the samples is most likely due to the fact that in the iron oxide layer for $Fe_2O_3/GaN/Al_2O_3$ crystals retain a structure close to a maghemite, that is, a cubic one. Maghemite is unstable at elevated temperatures and oxidizes to hematite, but it can partially survive inside these cubic grains. In terms of the magnitude of M_s and the ratios of M_{rs}/M_s and H_{cr}/H_c, as well as X-ray spectral and X-ray phase analysis data, the obtained iron oxide layers are similar in magnetic properties to hematite. The effect of maghemite is insignificant in the increase of M_s and M_{rs} for the sample $Fe_2O_3/GaN/Al_2O_3$ (see Table 2). This can be explained by the small volume of the core (maghemite) relative to the volume of the shell (hematite) in grains of the „core-shell“ type.

At room temperature, hematite is a weak ferromagnet and should be in the MD state in the case of bulk samples [6]. It was proven in Ref. [6] that the transition from the SD state directly to the MD state takes place in the case of bulk hematite crystals. In the case of submicron layers, hematite in a zero external field can be in the SV state [7] with a characteristic size of magnetic vortices of the order of 100−1000,nm. Therefore, it can be assumed that the submicron layers we are studying must contain these vortex structures in one form or another.

The MFM images (Figure 3) show areas of scattering of magnetic fields. Magnetically inhomogeneous bands with a width of the order of 2μm can be distinguished in the case of the sample of Fe_2O_3/Al_2O_3 (Figure 3, *a*), consisting of separate sections (in the form of „humps“ and „depressions“) of the same order in size and representing vortex magnetic structures. In the case of the sample of $Fe_2O_3/GaN/Al_2O_3$ (Figure 3, *b*), areas similar to magnetic domains having characteristic sizes of the order of 2μm and representing vortex magnetic structures. In the absence of an external field, these regions can be considered as separate magnetostatically interacting particles with effective spontaneous magnetization $I_{rs\,eff}$ [10].

The effective magnetization can be estimated from the remanent magnetization $I_{rs\,eff}$ using the formula: $C_{rs} \cdot I_{rs\,eff} = C_s \cdot I_{s\,eff} \cdot (M_{rs}/M_s)$, where $I_{s\,eff}$ is the effective spontaneous saturation magnetization; C_s is the volume concentration of ferromagnet; C_{rs} is the volume concentration of ferromagnet contributing to remanent magnetization [9.10]. We assume that the volume concentrations of the ferromagnet in the iron oxide layer C_{rs} and C_s are approximately equal to 1. For the sample Fe_2O_3/Al_2O_3 $I_{s\,eff} = I_s = 2.5$ kA/m [11]. Then $I_{rs\,eff} = 0.15$ kA/m. For the sample $Fe_2O_3/GaN/Al_2O_3$, the saturation magnetization value M_s is 1.4 times higher than for the sample Fe_2O_3/Al_2O_3 (see Table 2). Then $I_{s\,eff} \approx 3.5$ kA/m. Therefore, $I_{rs\,eff} = 0.31$ kA/m. Taking into account the fact that the spontaneous magnetization of maghemite (see, for example, [12]) is about 150 times greater than that of hematite, its volume concentration is no more than a few percent.

Since the characteristic value of $M_{rs}/M_s \approx (0.5-0.9)$ [5] for bulk hematite samples and the transition between the SD and MD states takes place bypassing the SV [6] state, the small values of $I_{rs\,eff}/I_{s\,eff} \approx M_{rs}/M_s \sim 0.06-0.09$for our samples indicate the presence of vortex structures [7].

4. Conclusion

A study of the magnetic properties of submicron layers of iron-III oxide obtained by the mist-CVD method on sapphire without a buffer layer (Fe_2O_3) and with a buffer layer of gallium nitride (Fe_2O_3/GaN), allowed determining the key features of their crystal structure and magnetic state. Both samples exhibit characteristics close to hematite (α-Fe_2O_3), however, the presence of a GaN buffer layer and the presence of a maghemite phase (γ-Fe_2O_3) in the sample $Fe_2O_3/GaN/Al_2O_3$ leads to an increase in saturation magnetization ($M_s = 46\,\mathrm{mA}\cdot\mathrm{m}^2/\mathrm{kg}$) compared to Fe_2O_3/Al_2O_3 ($M_s = 33\,\mathrm{mA}\cdot\mathrm{m}^2/\mathrm{kg}$). This may be due to the oxidation of maghemite to hematite with the preservation of γ-Fe_2O_3 core inside the grains, as well as the diffusion of Ga and N atoms into the iron oxide layer and the crystallographic effect of GaN, which modifies the magnetic sublattices of hematite.

The results obtained by magnetic force microscopy, magnetometric data, and theoretical estimates suggested the presence of vortex magnetic structures in the studied submicron layers, which is consistent with the literature data. A band structure containing localized magnetic inhomogeneous regions with characteristic dimensions $\sim 2\,\mu$m is observed in Fe_2O_3/Al_2O_3, whereas the distribution of regions is chaotic in $Fe_2O_3/GaN/Al_2O_3$, which can be explained by interfacial stresses. The values of the ratios $M_{rs}/M_s = 0.06-0.09$ and $H_{cr}/H_c = 1.2-1.5$ confirm the presence of vortex magnetic configurations. The results obtained show the dependence of the magnetic properties of the submicron layers of iron oxides on their crystal structure and morphology.

Acknowledgments

The work was performed using the equipment of the resource centers of the St. Petersburg State University Science Park: „Nanotechnology“; „Center for Microscopy and Microanalysis“; „Innovative technologies of composite nanomaterials“.

Conflict of interest

The authors declare that they have no conflict of interest.

References

[1] L. Machala, J. Tucek, R. Zboril. Chem. Mater. **23**, 3255 (2011).
[2] K.G. Gareev. Magnetochemistry **9**, 119 (2023).
[3] H. Zhang, B. Xia, D. Gao. J. Magn. Magn. Mater. **569**, 170428 (2023).
[4] R. Garg, S. Gonuguntla, S. Sk, M.S. Iqbal, A.O. Dada, U. Pal, M. Ahmadipour. Adv. Colloid Interface Sci. **330**, 103203 (2024).
[5] Ö. Özdemir, D.J. Dunlop. J. Geophys. Res. Solid Earth. **119**, 2582 (2014).
[6] A.P. Roberts, X. Zhao, P. Hu, A. Abrajevitch, Y.-H. Chen, R.J. Harrison, D. Heslop, Z. Jiang, J. Li, Q. Liu, A.R. Muxworthy, H. Oda, H.St.C. O'Neill, B.J. Pillans, T. Sato. J. Geophys. Res. Solid Earth **126**, e2021JB023027 (2021).
[7] F.P. Chmiel, N. Waterfield Price, R.D. Johnson, A.D. Lamirand, J. Schad, G. van der Laan, D.T. Harris, J. Irwin, M.S. Rzchowski, C.-B. Eom, P.G. Radaelli. Nature Mater. **17**, 581 (2018).
[8] V.I. Nikolaev, R.B. Timashov, A.I. Stepanov, S.I. Stepanov, A.V. Chikiryaka, M.P. Shcheglov, A.Ya. Polyakov. Pis'ma v ZhTF **49**, *10*, 43 (2023) (in Russian).
[9] P.V. Kharitonskii, E.A. Setrov, A.Yu. Ralin. Mater. Phys. Mech. **52**, *2*, 142 (2024).
[10] P.V. Kharitonsky, V.I. Nikolaev, V.M. Krymov, R.B. Timashov, E.S. Sergienko, D.D. Dubeshko, K.G. Gareev, A.Yu. Ralin. FTT **66**, *11*, 1902 (2024) (in Russian).
[11] D.J. Dunlop. Ann. Géophys. **27**, 269 (1971).
[12] B.M. Moskowitz, R.B. Frankel, S.A. Walton, D.P. Dickson, K.K.W. Wong, T. Douglas, S. Mann. J. Geophys. Res. Solid Earth **102**, *B10*, 22671 (1997).

Translated by A.Akhtyamov